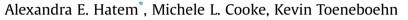
Journal of Structural Geology 101 (2017) 96-108

Contents lists available at ScienceDirect

Journal of Structural Geology

journal homepage: www.elsevier.com/locate/jsg

Strain localization and evolving kinematic efficiency of initiating strike-slip faults within wet kaolin experiments



Department of Geosciences, University of Massachusetts Amherst, Amherst, MA, USA

A R T I C L E I N F O

Article history: Received 3 November 2016 Received in revised form 22 June 2017 Accepted 27 June 2017 Available online 29 June 2017

Keywords: Kinematic efficiency Strike-slip initiation Strain localization Analog modeling Shear zone evolution Off-fault deformation

ABSTRACT

Using wet kaolin experiments, we document the evolution of strain localization during strike-slip fault maturation under variable boundary conditions (pre-existing fault, depth of and distribution of basal shear). While the nature of the basal shear influences strain localization observed at the clay surface, similarities between experiments reveal a general conceptual model of strain accommodation. First, shear strain is accommodated as distributed shear (Stage 0), then by development of echelon faults (Stage I), then by interaction, lengthening and propagation of those echelon faults (Stage II) and, finally, by slip along through-going fault (Stage III). Stage II serves as a transitory period when the system reorganizes after sufficient strain localization. Here, active fault system complexity is maximized as faults link producing apparent rotation of active fault slip and kinematic efficiency increases. We quantify kinematic efficiency as the ratio of fault slip to applied displacement. All fault systems reach a steady-state efficiency in excess of 80%. Despite reducing off-fault deformation, the through-going fault maintains <1.5 cm structural irregularities (i.e., stepovers), which suggests that small (<3 km) stepovers may persist along mature, efficient faults in the crust.

© 2017 Elsevier Ltd. All rights reserved.

1. Introduction

As strike-slip faults initiate and mature in the upper crust, field and modeling studies suggest that echelon fractures (opening and sliding mode cracks) form first, and eventually link to form a continuous strike-slip fault (e.g., Cloos, 1928; Riedel, 1929; Tchalenko, 1970; Wilcox et al., 1973; Segall and Pollard, 1983; Wesnousky, 1988; An and Sammis, 1996; Stirling et al., 1996; Ben-Zion and Sammis, 2003; Crider and Peacock, 2004). Once these cracks have linked, strike-slip can occur along a narrow zone, with abandoned early fractures surrounding the fault core (e.g., Caine et al., 1996; Shipton and Cowie, 2001, 2003; Zinke et al., 2015).

For instance, Chester and Chester (1998) documented that most slip occurs along a thin principal fault within an ultracatclasite gouge layer along the Punchbowl fault. They noted many fractures surrounding the principal fault that accommodated two orders of magnitude less slip than the principal fault (<100 m distributed slip within damage about the fault versus 40 + km on the whole fault).

Because of this marked partitioning of total slip, Chester and Chester (1998) inferred that early distributed strain throughout the fault zone must have localized over small amounts of applied strain. The thin, localized nature of the Punchbowl fault is consistent with the inference that the mature fault, when active, must have accommodated most of the plate boundary strain.

Crider and Peacock (2004) compiled observations similar to that of Chester and Chester (1998) and synthesized a conceptual model of four stages of strain localization. Although they found that some faults grow from reactivation of pre-existing faults, Crider and Peacock (2004) showed that most faults grow from linkage of precursory structures. When faults grew from precursory structures, Crider and Peacock (2004) defined three stages of fault growth: the first stage is shear along such precursory structures, the second stage is linkage of the shear fractures via new structures that grow under a new stress field as the fault zone develops, and the third stage is slip along a through-going fault composed of these linked structures.

Laboratory studies of strike-slip fault development by Tchalenko (1970) support the field observations made by Chester and Chester (1998) and the stages of fault initiation synthesized by Crider and Peacock (2004). By mapping photographs of analog experiments





JUBRAL OF STRUCTURAL GEOLOGY

^{*} Corresponding author. Now at: Department of Earth Sciences, University of Southern California, 3651 Trousdale Parkway, Los Angeles, CA, 90089, USA. *E-mail address: ahatem@usc.edu* (A.E. Hatem).

in kaolin (analogous to mapping from air photos), Tchalenko (1970) documented the first-order kinematics of strike-slip fault evolution and showed that echelon fractures not only grow at peak strength of the kaolin, but also serve as precursory structures for a throughgoing fault. Tchalenko (1970)'s stages of strike-slip fault development, framed by the evolution of force during experiments, resemble the stages later developed by Crider and Peacock (2004) using field observations. Tchalenko's first stage occurs up to the peak shear resistance (i.e., force) associated with echelon fault growth, the second stage starts after the peak force was reached, as stress was relieved by the growth of another set of oblique, echelon shears, and the third stage is continued weakening of the fault zone as stresses decrease with the development of a principal fault surface.

These previous studies leave questions unanswered about the nature of early slip localization during strike-slip fault initiation. Do the echelon precursory structures develop only during the initial evolution of shear zones, or do they continue to grow throughout the fault's evolution? How do these precursory structures evolve structurally and mechanically to form a relatively simple throughgoing fault? How do boundary conditions, such as basal shear nature and depth, affect strike-slip fault development observed at the surface? Our study addresses these questions by directly recording details of strain localization throughout the development of strikeslip faults using innovative experimental techniques. We improve upon the previous experiments of Tchalenko (1970) by using rigorously scaled material and increasing sampling resolution of deformation (i.e., shear strain), both in space and in time throughout the experiment. High-resolution digital image correlation techniques allow us to record the evolution of shear strain distribution, active shear zone width, fault complexity and kinematic efficiency throughout the early development of strike-slip faults in finer detail than in previous analog studies. Here, we define kinematic efficiency as the portion of applied velocity that is expressed as incremental slip along the faults (e.g., Cooke et al., 2013; Hatem et al., 2015). Kinematically efficient fault systems have greater fault slip and less off-fault deformation. As faults propagate to develop linked, through-going surfaces, their kinematic efficiency increases (Cooke et al., 2013; Hatem et al., 2015). Consequently, mature faults should be more efficient than immature faults and require less work to maintain deformation, as strain has fully localized onto a primary fault or group of primary faults (e.g., Cooke and Murphy, 2004; Newman and Griffith, 2014; Cooke and Madden, 2014). The increase in kinematic efficiency during fault evolution corresponds to the decrease in shear resistance (i.e., force), which was directly measured by Tchalenko (1970). Additionally, in order to investigate the dependency of strain localization and kinematic efficiency evolution on faulting conditions, we vary boundary conditions to investigate different distributions of basal shear, depths of basal shear zones and reactivation of preexisting faults. These boundary conditions aim to assess the effect of basal shear and fault conditions on the nature of strike-slip fault maturation and evolution of kinematic efficiency. Like previous studies, we observe discrete stages of strike-slip fault evolution. This study demonstrates four stages of strain localization observed from surface measurements as strike-slip faults mature: (0) distributed shear antecedent to shear localization; (I) localization of strain either onto new small echelon faults or onto pre-existing faults; (II) interaction and reorganization of echelon faults; and (III) localized strike-slip along a through-going fault.

2. Methods

Scaled physical experiments with wet kaolin lasting just a few hours in a laboratory allow us to understand crustal processes that typically span millions of years over large spatial regions. Furthermore, the deformation and evolving maturity of strike-slip faults within scaled physical experiments can be directly observed and measured, whereas we can only infer such deformation from field observations. In this study, we used scaled experiments within wet kaolin to simulate the initiation and maturation of crustal strikeslip faults. Through carefully scaling the strength of the clay and the length scales of the claybox, we apply results from the claybox to crustal fault systems.

2.1. Wet kaolin

The experiments grew faults within wet kaolin, with ~65–75% water by mass, as have many previous fault evolution studies (e.g., Eisenstadt and Sims, 2005; Schlische et al., 2002; Henza et al., 2010; Cooke et al., 2013; Hatem et al., 2015). Following AASHTO T-88 10 and ASTM D422-63 standard methods for particle size analysis of soils, we determined the silt and clay grain size distribution of the kaolin used in the experiments of this study, as well as the percent of grains coarser than 62 µm (sand). Our kaolin consists of 5–10% sand, 30–35% silt, and 60% clay-sized particles by mass. Unlike dry sand, which is often used in crustal simulations of deformation, wet kaolin grows discrete hairline faults and the fault surfaces can be reactivated in different loading conditions (e.g., Withjack and Jamison, 1986; Bonini et al., 2015). These characteristics make wet kaolin an ideal material for studying fault evolution as faults are long-lived until they become mechanically unfavored. The observed reactivation of faults in wet kaolin under a wide range of loading, suggests that the faults have low residual strength (e.g. Henza et al., 2010; Hatem et al., 2015). The coefficient of internal friction, evident from dip of faults under extension, is equitable to that of the Earth's crust (~0.7) (Henza et al., 2010).

Like crustal material, wet kaolin deforms as a bi-viscous Burger's material with both elastic and viscous properties (Cooke and van der Elst, 2012). The experiments are all run with plate velocity of 0.5 mm per minute and the experiments typically run for 2 h. Because the Maxwell relaxation time of the wet kaolin is 15 min, the material exhibits significant viscous deformation as does the Earth's crust over several millions of years of fault evolution; upper crust viscosity of 10²⁴ Pa-sec yields Maxwell relaxation time of 2.1 Ma. The 2-h experiments simulate the evolution of crustal strikeslip faults over ~16 Ma years.

The shear strength of wet kaolin can be manipulated by altering the water content in order to scale the wet kaolin experiments to the strength and length of the Earth's crust. Some previous experiments use moist clay with a lower water content (60%) than our experiments (65–75%) (e.g., Tchalenko, 1970; An and Sammis, 1996; Curren and Bird, 2014). Using a drier clay will have correspondingly higher shear strength (Eisenstadt and Sims, 2005). The density of the wet kaolin in the experiments discussed here is ~1.6 g/cm³. We modify the water content of the wet kaolin so that fall cone strength tests (DeGroot and Lunne, 2007) show shear strengths of 100–110 Pa. If we consider a density of continental crust of 2.65 g/cm³ and crustal shear strength of 10–20 MPa, the length scaling is 1 cm in the claybox to 0.5–1.2 km of continental crust. We calculate this length scaling ratio by the following equation:

$$\frac{S_m}{S_p} = \frac{\rho_m}{\rho_p} \frac{z_m}{z_p} \tag{1}$$

In Equation (1), the strength (*S*) ratio of model (*m*) to prototype (*p*) is equal to the density (ρ) ratio multiplied by the length (*z*) ratio (e.g., Henza et al., 2010). Over the several hours of a typical experiment we observe only ~2% water loss, which correlates to

Download English Version:

https://daneshyari.com/en/article/5786292

Download Persian Version:

https://daneshyari.com/article/5786292

Daneshyari.com